AGU PUBLICATIONS

JGR

Journal of Geophysical Research: Space Physics

RESEARCH ARTICLE
10.1002/2015JA021409

Key Points:
- Larger winter activity East of Andes is found from stratosphere to ionosphere
- It may be useful to separate night and day cases to study GWs in the ionosphere
- Orographic GWs may not usually become likely absorbed in the neutral atmosphere

Correspondence to:
P. Alexander,
peter@df.uba.ar

Citation:
Alexander, P., A. de la Torre, T. Schmidt, P. Llamedo, and R. Hierro (2015), Limb sounders tracking topographic gravity wave activity from the stratosphere to the ionosphere around midlatitude Andes, *J. Geophys. Res. Space Physics*, *120*, doi:10.1002/2015JA021409.

Received 11 MAY 2015
Accepted 25 SEP 2015
Accepted article online 1 OCT 2015

Limb sounders tracking topographic gravity wave activity from the stratosphere to the ionosphere around midlatitude Andes

P. Alexander[1], A. de la Torre[2], T. Schmidt[3], P. Llamedo[2], and R. Hierro[2]

[1]Instituto de Física de Buenos Aires, Conicet, Ciudad Universitaria Pabellón 1, 1428 Buenos Aires, Argentina, [2]Facultad de Ingeniería, Universidad Austral, Pilar, Argentina, [3]Helmholtz Centre Potsdam, GFZ German Research Centre for Geosciences, Potsdam, Germany

Abstract Several studies have shown that the surroundings of the highest Andes mountains at midlatitudes in the Southern Hemisphere exhibit gravity waves (GWs) generated by diverse sources which may traverse the troposphere and then penetrate the upper layers if conditions are favorable. There is a specific latitude band where that mountain range is nearly perfectly aligned with the north-south direction, which favors the generation of wavefronts parallel to this orientation. This fact may allow an optimization of procedures to identify topographic GW in some of the observations. We analyze data per season to the east and west of these Andes latitudes to find possible significant differences in GW activity between both sectors. GW effects generated by topography and convection are expected essentially on the eastern side. We use satellite data from two different limb sounding methods: the Global Positioning System radio occultation (RO) technique and the Sounding of the Atmosphere using Broadband Emission Radiometry instrument, which are complementary with respect to the height intervals, in order to study the effects of GW from the stratosphere to the ionosphere. Activity becomes quantified by the GW average potential energy in the stratosphere and mesosphere and by the electron density variance content in the ionosphere. Consistent larger GW activity on the eastern sector is observed from the stratosphere to the ionosphere (night values). However, this fact remains statistically significant at the 90% significance level only during winter, when GWs generated by topography dominate the eastern sector. On the contrary, it is usually assumed that orographic GWs have nearly zero horizontal phase speed and will therefore probably be filtered at some height in the neutral atmosphere. However, this scheme relies on the assumption that the wind is uniform and constant. Our results also suggest that it is advisable to separate night and day cases to study GWs in the ionosphere, as it is more difficult to find significant statistical differences during daytime. This may happen because perturbations induced by GWs during daytime are more likely to occur in a disturbed environment that may hinder the identification of the waves.

1. Introduction

The interpretation of ionospheric irregularities in terms of gravity waves (GWs) propagating from the lower atmosphere was introduced by *Hines* [1960]. Thereafter, observations, theoretical studies, and models inferred the conditions that allow the upward GW propagation and the generation of secondary GW due to nonlinear interactions or wave dissipation [see, e.g., *Vadas et al.*, 2003; *Lund and Fritts*, 2012; *Vadas and Liu*, 2013]. Some observations have revealed that traveling ionospheric disturbances might be GW propagation manifestations [see, e.g., *Hocke and Schlegel*, 1996]. The presence of GWs or their effects has been observed or modeled up to about 500 km altitude or even higher [see, e.g., *Park et al.*, 2014; *Vadas et al.*, 2014]. There is general agreement that the primary GW sources are present in the lower neutral atmosphere. In relation to the effects in the ionosphere, most attention has focused on GWs generated by deep convection [see, e.g., *Hocke and Tsuda*, 2001], because it is able to yield large-scale GWs with significant phase speeds, as the latter condition is sufficient (although not necessary) to penetrate the lower ionosphere to avoid removal through critical level filtering and instability dynamics [see, e.g., *Fritts and Lund*, 2011; *Lund and Fritts*, 2012]. Other lower atmosphere GW sources, such as orography and jet stream winds and shears, apparently lead to phase speeds that would significantly reduce the probability of penetration into the ionosphere. However, we would like to challenge this assertion at least in reference to mountain waves, as there are two core assumptions [see, e.g., *Baines*, 1995]

which are often overlooked: usually, the impinging wind is neither uniform nor constant. Any situation where both characteristics break down should lead to nonstationary GWs as seen from the ground. This fact implies that upward propagation of orographic GWs might in some cases avoid critical level filtering and could thus be detected in the ionosphere.

Some ground, balloon, airglow, satellite, and numerical modeling studies have shown that the surroundings of the highest Andes mountains at midlatitudes in the Southern Hemisphere constitute a natural laboratory where GWs generated by topography around winter and by convection around summer, as well as by geostrophic adjustment and instability, may traverse the troposphere and upper layers [*de La Torre et al.*, 1994; *Reisin and Scheer*, 2004; *de la Torre and Alexander*, 2005; *Llamedo et al.*, 2009; *Smith et al.*, 2009]. These studies mostly focused on specific height intervals, so a follow-up analysis on GW effects across various atmospheric layers in this region may provide a more comprehensive view on their possible upward penetration. The stratospheric polar vortex is also a well-known GW source above Antarctica and the surrounding region, whereby the activity peaks during the spring decay of the jet [see, e.g., *Alexander et al.*, 2009; *Moffat-Griffin et al.*, 2013]. However, although these GWs tend to be significant, they are not adequate for our study because we cannot foresee such a simple identification and localization. For example, the vortex exhibits latitudinal excursions which may sometimes even reach the southernmost part of the continent and in addition it can partially reflect upward propagating GWs from tropospheric sources [*Sato et al.*, 2012].

In April 2006, the Constellation Observing System for Meteorology, Ionosphere, and Climate (COSMIC) launched six satellites to use the Global Positioning System (GPS) radio occultation (RO) technique to measure different atmospheric properties in the troposphere, stratosphere, and ionosphere [e.g., *Liou et al.*, 2007; *Anthes*, 2011]. The aim of the mission was to produce up to 2500 daily soundings with global distribution. It is presently still obtaining vertical profiles of temperature, pressure, refractivity, and water vapor in the neutral atmosphere and electron density in the ionosphere. The present study uses postprocessed data (product version 2010.2640) from the COSMIC mission provided by COSMIC Data Analysis and Archive Center. We use the vertical profiles of temperature in the neutral atmosphere and electron density in the ionosphere to evaluate GW activities to the east and west of Andes at midlatitudes in the Southern Hemisphere and find out possible differences between them. GWs which produce more significant effects to the east of the mountains could be due to topography or convection, but as both sources typically operate during different seasons, any activity differences could be eventually ascribed to a given mechanism. There exist just a few studies that combine GPS RO data in the neutral atmosphere and ionosphere to study possible links between both regions. *Yue et al.* [2010] and *Lin et al.* [2012a, 2012b, 2013] studied the effects of stratospheric sudden warming events in the ionosphere by analyzing the corresponding response of diverse parameters of the electron density profiles and the modification of tidal signatures in that layer. On the other hand, *Hocke and Tsuda* [2001], *Hocke et al.* [2002], *Tsuda and Hocke* [2004] looked for possible consequences of the propagation of stratospheric GWs into the ionosphere and observed that those modes were highly correlated with sporadic layers and other irregularities in the *E* region above the tropical convection zones and the Southern Andes.

To complete the data gap from the upper stratosphere to the mesosphere, we also use profiles from the SABER (Sounding of the Atmosphere using Broadband Emission Radiometry) instrument [e.g., *Mlynczak*, 1997]. SABER is an infrared emission limb sounder covering the upper troposphere, stratosphere, mesosphere, and lower thermosphere and is on board the Thermosphere Ionosphere Mesosphere Energetics and Dynamics satellite. Here we use kinetic temperatures from version 2.0 retrievals. SABER and GPS RO possess a similar observational filter in reference to the horizontal and vertical resolutions.

Section 2 describes the GPS RO and SABER data and their transformation into GW activity assessments in the studied atmospheric layers. In section 3, we present the results. We intend to track GW signatures from the stratosphere to the ionosphere, in order to determine if there is an observable differential activity above the eastern side of the Andes Mountains around specific seasons. Conclusions are then presented in section 4.

2. Data and Analysis Method

We considered all COSMIC and SABER events within the zone limited by latitudes 29–36°S and longitudes 65–75°W. The time span used for GPS RO and SABER data was between 1 July 2006 and 31 December 2013. There were 2937 GPS RO retrievals in the ionosphere and 5958 in the neutral atmosphere and 5295 SABER profiles. The Andes mountains are nearly perfectly aligned with the meridian 70°W in the geographic region under analysis (see Figure 1). The zone was then divided in two sectors: to the east and to the west of that

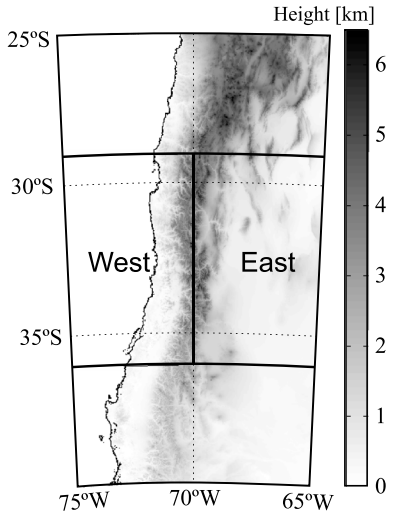

Figure 1. The two sectors under study and the topography dividing them about 70°W between 29°S and 36°S.

longitude. Results were separated in seasons of the Southern Hemisphere: summer (December-January-February), autumn (March-April-May), winter (June-July-August), and spring (September-October-November). For our calculations, we used the GPS RO temperature and electron density profiles, respectively, in the lower stratosphere and ionosphere and SABER temperature retrievals in the stratosphere and mesosphere.

GPS RO can optimally detect inertio-GW, but it is possible to improve the observation of mountain waves signatures [*Alexander et al.*, 2008]. The line of sight (LOS) of the retrievals has a horizontal orientation at every tangent point. If the LOS is nearly perpendicular to the horizontal projection of any present wavefronts, then only a weak signature or none will be detected, because the integrated measure along the observational path will encompass successive positive and negative contributions of the wave, which will nearly cancel out the final outcome. On the other hand, if the LOS is nearly parallel to the wavefronts, then the smearing along the observational path is roughly performed on constant phase surfaces and no cancelations will likely occur. This is an optimal situation for GW detection because fluctuations become preserved by the retrieval. GW fronts generated by topography will be preferentially aligned with it [*Baines*, 1995]. In the geographical region that we study, this applies to the north-south direction [e.g., *Llamedo et al.*, 2009], which will make GWs more suitable for detection by GPS RO if we discard the LOS in the neutral atmosphere around the west-east orientation, because they would then be likely perpendicular to the expected horizontal component of the wavefronts. Close to the region under study *Alexander et al.* [2009] found that about 41% of COSMIC RO had a LOS within 30° of the north-south direction. This preferential meridional alignment of the LOS is advantageous regarding the detection of GWs originated by the Andes, as corroborated by *Baumgaertner and McDonald* [2007] around the Antarctic Peninsula. LOS were restricted in our study to $\pm$ 60°from the north-south direction. This limitation also included the ionospheric retrievals, in order to avoid the inclusion of some soundings where measurements along the LOS might be simultaneously sampling the east and west sectors.

We calculated the potential energy per unit mass E_p for each individual sounding in the neutral atmosphere and then assessed GW activity per season, sector, and layer by the corresponding mean value. E_p was calculated through the average relative temperature T variance of each profile between altitudes z_1 and z_2 [*Wilson et al.*, 1991]

$$E_p = \frac{1}{z_2 - z_1} \int_{z_1}^{z_2} \frac{1}{2} \left(\frac{g}{N}\right)^2 \left(\frac{T'}{T_b}\right)^2 \mathrm{d}z \tag{1}$$

where g is the gravitational acceleration and N represents the Brunt-Väisälä frequency, which may be derived from each temperature profile. The ratio of perturbation and background temperatures T'/T_b was obtained as follows in each case. For GPS RO retrievals, the T profiles were low-pass filtered, with a wavelength cutoff at 12 km, obtaining T_b. The filter is nonrecursive, and a Kaiser window was used [e.g., *Hamming*, 1998]. It was applied again to the difference $T - T_b$ with a cutoff at 3 km, as the GPS RO vertical resolution is about 1.4 km in the stratosphere [*Kursinski et al.*, 1997]. This procedure gives T' profiles which isolate wavelengths between 3 and 12 km. The z_1 to z_2 vertical column for the integral was 19 to 31 km (i.e., lower stratosphere in this region). Higher altitudes from GPS RO data should not be used to infer GWs [*Luna et al.*, 2013]. These authors have shown that RO temperature profiles are less reliable for GW E_p calculations above about 30 km. The possible origin of this artifact is that spurious oscillations introduced by the initialization procedure of GPS RO atmospheric retrievals have a significant presence up to approximately 30 km. This may inject artificial additional E_p to the profiles above that height. Although tropospheric data are available, it is standard use to study only the stratosphere because a problem arises around the tropopause, as the sharp change in temperature gradient sign leads to an artificial enhancement in wave activity when using digital filters to isolate wave components [e.g., *Schmidt et al.*, 2008; *de la Torre et al.*, 2010]. SABER can detect vertical wavelengths above 5 km

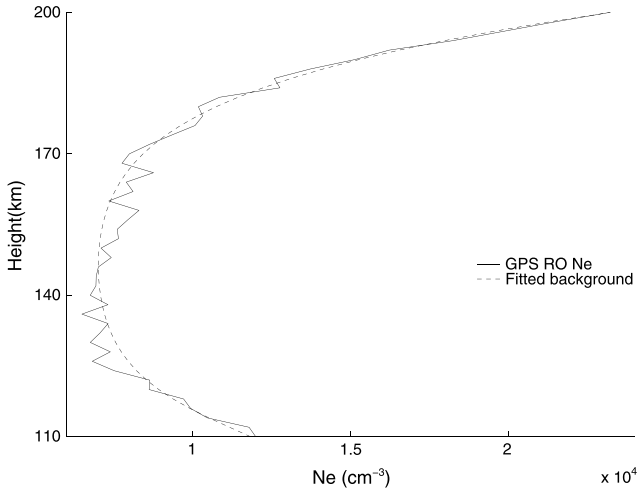

Figure 2. A GPS RO electron density profile chosen among the analyzed retrievals and the corresponding background fitted by a double Chapman layer.

[*John and Kumar*, 2012], so we isolated in these profiles the modes between 5 and 20 km with the same filter. The vertical columns in the stratosphere and mesosphere were, respectively, taken from 20 to 40 km and from 55 to 75 km to avoid the same digital filter problem in the stratopause and mesopause as in the tropopause. The described procedure does not specifically remove planetary waves, but *McDonald et al.* [2010] and *Alexander et al.* [2011] have shown that the effects due to GWs are generally much larger than those due to planetary waves.

It will be shown below that it is highly convenient to separate day and night cases for ionospheric activity calculations, as the conditions and perturbation state may be quite different for both time intervals. If this classification is not made, one might mix different categories. We discarded cases with unphysical negative electron density N_e [e.g., *Høeg et al.*, 1998] and also cases with sporadic *E* layers, as they could strongly affect activity estimations. GPS RO electron density profiles have a vertical resolution about 1.5 km [*Schreiner et al.*, 1999]. To separate the background and perturbation components in each profile, we used a double Chapman layer to model the *E* and *F* regions [e.g., *Bilitza*, 2002]. Background fits that did not match the similarity criterium with the original profile through the coefficient of determination $R^2 > 0.8$ were discarded. It is implicitly assumed that perturbations induced by the GWs are moderate or small and that R^2 will then measure the quality of the fit to the large-scale behavior, rather than to the small-scale activity features. As a typical example of the separation procedure of background and fluctuations, in Figure 2 we show one of the N_e profiles used for our study and the background fitted according to the double Chapman layer equation. Using the same filtering procedure as described above, we obtained the electron density perturbation δN_e by keeping only wavelengths in the range between 3 and 20 km (to retain only the fluctuations likely induced by GWs). In order to quantify ionospheric GW activity, we considered two possible proxies [*de la Torre et al.*, 2014]: the mean relative variance content from a total of *M* electron density profiles

$$\mathrm{MRVC} = \frac{1}{M(z_2 - z_1)} \sum_{k=1}^{M} \int_{z_1}^{z_2} \left(\frac{\delta N_{e_k}}{N_{eb_k}} \right)^2 \mathrm{d}z \tag{2}$$

and the mean absolute variance content

$$\mathrm{MAVC} = \frac{1}{M(z_2 - z_1)} \sum_{k=1}^{M} \int_{z_1}^{z_2} (\delta N_{e_k})^2 \mathrm{d}z \tag{3}$$

where z_1 and z_2 in this case are 110 and 200 km and N_{eb_k} refers to the background electron density. MRVC may seem a priori, a more appropriate measure, as it takes into account the tendency of N_e to increase with altitude, weighting the relative importance of the perturbation component with respect to the background profile. However, some retrieved RO N_e profiles may display negative biases. This error may lead to division by close to null values, resulting in unrealistic estimations in MRVC. We chose our lower level at 110 km to avoid most sporadic *E* layers. Although GWs or their effects have been observed as high as about 500 km as recalled above, our upper level was chosen at 200 km. Higher altitudes could lead in general to wrong results, after a declining importance of the upward propagating GWs and their effects in favor of other important phenomena causing perturbations. Another aspect which should be considered is the fact that vertical wavelengths tend to become larger with increasing altitude in the lower thermosphere because of the effects of kinematic viscosity and thermal diffusivity [*Vadas*, 2007]. If the corresponding horizontal wavelengths typically become larger in a lower proportion, stay the same or if they decrease, then the observation of GWs by GPS RO would

Table 1. Mean GW Activity to the West/East of the Andes Mountains Per Season and the Number N_s of Soundings Used in the Calculations[a]

Season	N_s	Activity (J/kg)		
	Lower Stratosphere (*GPS RO Data*)			
Summer	585/559	0.994[c]/1.01[c]		
Autumn	585/489	0.879/1.17[c,b]		
Winter	497/476	0.901/1.36[c,b]		
Spring	578/581	0.867[c]/0.957[b]		
	Stratosphere (*SABER Data*)			
Summer	667/632	5.45/5.73[b]		
Autumn	590/594	5.54[c]/5.81[c,b]		
Winter	619/673	8.85[c]/9.90[c,b]		
Spring	784/736	6.41[c]/6.73[c,b]		
	Mesosphere (*SABER Data*)			
Summer	667/632	14.5[c]/14.8[c]		
Autumn	590/594	13.4[c]/13.7[c]		
Winter	619/673	19.0[c]/19.9[c,b]		
Spring	784/736	13.8[c]/14.1[c]		
	Ionosphere (*GPS RO Data*)			
		Absolute Activity (cm^{-6})		Relative Activity
			Day	
Summer	102/104	6.59e+07[c]/4.58e+07[c]		0.0042[c]/0.0034[c]
Autumn	140/71	2.48e+08[c]/1.75e+08		0.0064/0.0059
Winter	122/91	1.51e+08[c]/1.93e+08[c,b]		0.0062[c]/0.0053[c]
Spring	143/107	7.84e+07[c]/7.91e+07[c]		0.0039/0.0037
			Night	
Summer	21/19	6.06e+06/6.81e+06		0.0032[c]/0.0039
Autumn	73/62	7.00e+06/4.33e+06[c]		0.0079/0.0031[c]
Winter	56/56	5.23e+06/1.22e+07[b]		0.0084[c]/0.0120[c,b]
Spring	29/20	4.87e+06/8.05e+06[b]		0.0023/0.0043[b]

[a]Absolute and relative mean GW activities are considered in the ionosphere, whereby day and night events are processed separately.
[b]The east value is significantly larger than the west value at the 90% level of confidence.
[c]The value is significantly different from the value of the following season at the 90% level of confidence.

worsen with growing height, as the optimal situation for detection is a low vertical to horizontal wavelength ratio [*Alexander et al.*, 2008]. For example, notice that in Figure 2 the fluctuations tend to disappear above about 190 km. Nevertheless, if this eventual problem exists, it should cause in each one of our average seasonal and geographical activity calculations in the ionosphere a similar collateral alteration. Specifically, it is expected that the final statistical effect would be the attainment of lower mean values, as GWs would be seen less clearly or not detected at all in an upper portion of the 110 to 200 km height range used here for all the profiles analyzed. However, this could not produce artificial higher average values. Then geographical or seasonal activity jumps could become masked but it is rather unlikely that spurious differences would emerge from the calculations.

To contrast neutral atmosphere and ionosphere activities, we chose to perform a climatological study as compared to the possible use of each GPS RO retrieval in the stratosphere and ionosphere for a correlation-type study between profiles of both height intervals. The reason is that due to the horizontal displacement of the GPS RO measurement points in each retrieval (typically a few 100 km), the observations in the ionosphere occur in a zone with different coordinates than in the lower stratosphere. Then in the analysis of every single GPS RO we might be observing the activity induced by some GWs in the lower atmosphere, but in the ionosphere we might not detect their effects, or vice versa. Also, due to technical issues, about one of every two

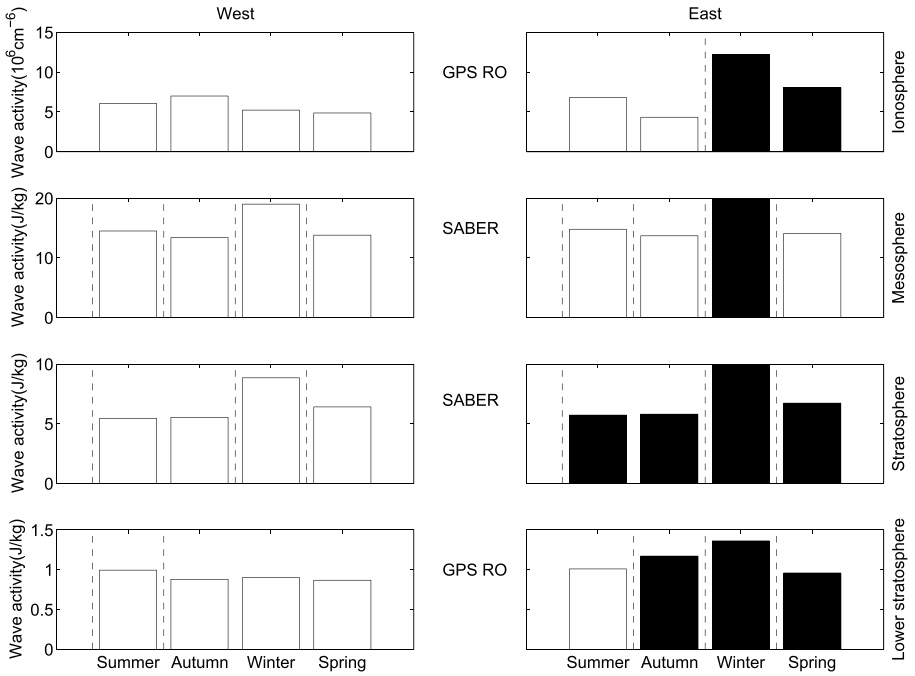

Figure 3. (bottom to top) Seasonal GW activity in the lower stratosphere, stratosphere, mesosphere, and ionosphere (nighttime absolute GW activity) calculated from GPS RO or SABER data. The black bars indicate that the eastern activity is significantly larger than the western one at the 90% confidence level. Dashed lines point out that the activities from adjacent seasons are significantly different at the 90% confidence level.

stratospheric retrievals becomes accompanied by a successful outcome in the ionosphere (see, for example, in the first paragraph of this section the amount of profiles in each of both layers in our study). Finally, GPS RO data miss the upper stratosphere and mesosphere regions.

3. Results

In the upper part of Table 1, we present the results for the mean GW activity per season in the lower stratosphere for the east and west sectors as obtained from GPS RO soundings. We evaluate if variations according to season or sector are significant. We assessed whether the differences between means were significant at the 90% level. In every case, we performed a *t* test. When testing differences between seasons, we performed a two-tailed test on the null hypothesis that both means are equal. When comparing the two neighboring sectors, we checked the null hypothesis that the activity in the east is lower than in the west. If the null hypothesis in the first case was rejected, we could state at the 90% statistical significance level that the means of successive seasons were different, and in the second case that the mean on the east side was larger than on the west side. Otherwise, we failed to reject both types of null hypotheses. Further down in Table 1, we repeated the procedure for the stratosphere and mesosphere from SABER retrievals. In the lowest part of Table 1, we present the calculations for the ionosphere from GPS RO data. We had to separate daytime and nighttime cases because the levels of activity change significantly in both situations. In Figure 3, we present a graphical scheme for the visualization and comparison of the GW activity results.

In the lower stratosphere, seasonal activity is significantly larger on the eastern side, with the only exception of summer. Then most of the observed GW activity in this sector and height interval is probably due to topography. GWs due to convection could be absent or may not be optimally visible to the observational window of GPS RO. In the whole stratosphere, differences between both sectors are significant for all seasons. In the mesosphere, all seasonal variations are significant, but differences between west and east are statistically remarkable only for winter. Seasonal behavior of mesospheric GW activity was obtained at altitudes 87 and 95 km from airglow measurements at El Leoncito (31.8°S, 69.2°W) during years 1998–2002 [*Reisin and Scheer* 2004]. It exhibited a main maximum in winter and a weaker maximum in summer. With our SABER data, we also see the summer minor maximum in the mesosphere. However, we must keep in mind that every measurement technique has its own filtering window, as it can only see a limited range of the full spectrum of

GWs. Therefore, a direct comparison of E_p values from GPS RO and SABER is not possible. In addition, *John and Kumar* [2012] and *Luna et al.* [2013] have shown that different processing of the same data or the use of observations from different satellites in the same region and time can lead to significant differences in the calculation of E_p. Statistically significant larger values of the ionospheric absolute and relative activity on the eastern side are observed during the night in winter and spring. We consider that GW effects are more clearly observed during the night, as the ionosphere may be in a more quiet state than during the day.

4. Conclusions

The main conclusion is that consistent differences regarding GW activity between the west and east sectors are observed from the stratosphere to the ionosphere (night values), but they all remain statistically significant at the 90% significance level only during winter. Spring and autumn tests fail in the mesosphere, and the latter season results also in the ionosphere. Winter is high season. We recall that significant GWs are mainly generated on the eastern side of the highest Andes Mountains due to flow over topography during winter. These GWs may reach considerable altitudes before breaking or finding critical levels or dissipating. It is usually assumed that topographic GWs have nearly zero horizontal phase speed and will therefore probably be filtered at some height in the neutral atmosphere. However, this notion relies on the assumption that the wind is uniform and constant. This situation may not be the typical one in the region under study. In our analysis, the observed ionospheric activity could be due to primary waves or to radiation of secondary waves. However, regarding the possible penetration of tropospheric waves into the ionosphere, larger amplitude oscillations below do not imply larger effects above. From numerical simulations, less intense GWs could more likely reach saturation and breaking levels at higher altitudes [e.g., *Fritts and Lund*, 2011].

de la Torre et al. [2014] did not include in the same studied region an evaluation of ionospheric activity in terms of seasons or its intensity in the lower layers. Both aspects are important because they can provide clues regarding the possible sources of the GWs affecting the ionosphere and the propagation, dissipation, or absorption processes that occur in the lower layers. In addition, although those authors already found higher activity on the east as compared to the west ionospheric sector without any discrimination between daytime and nighttime GPS RO data, our results suggest that it is advisable to separate both groups. There is clearly more difficulty in finding significant statistical differences during daytime than during nighttime, as in the former case perturbations induced by GWs may more likely occur in a disturbed environment that significantly deviates from a quiet background state, which may hinder the identification of the searched modes.

Data sets from different satellite instruments and/or heights may provide complementary statistical views on the generation and evolution of some portions of the whole spectrum of GWs. The possible detection of signatures depends in each case on the instrumental sensitivities to given parts of the wavelengths space. Different sources produce GWs that belong to diverse parts of the spectrum, but in addition, background winds may refract them into or out of the visibility range of given satellite sensors. Then, the statistical reconstruction with these tools may lead to a better understanding of GW generation and propagation during different seasons across different geographical regions, but for the moment the subject remains like a puzzle with missing pieces. In order to better investigate different parts of the whole GW spectrum, both satellite limb and nadir-observing techniques are needed in future work. These are respectively sensitive to small and large vertical to horizontal GW scale ratios, i.e., to low and high intrinsic frequencies as deduced from the dispersion relations for GWs [e.g., *Hines*, 1960]. Numerical simulations may also provide some of the missing pieces of the puzzle.

Acknowledgments
This manuscript is prepared under grant CONICET PIP11220120100034, ANPCYT PICT2013-1097, and German BMBF grant 01DN14001. P. Alexander, A. de la Torre, P. LLamedo, and R. Hierro are members of CONICET. GPS RO data are downloaded from cdaac-ftp.cosmic.ucar.edu, and SABER data from saber.gats-inc.com.

References

Alexander, P., A. de la Torre, and P. Llamedo (2008), Interpretation of gravity wave signatures in GPS radio occultations, *J. Geophys. Res.*, *113*, D16117, doi:10.1029/2007JD009390.

Alexander, S. P., A. R. Klekociuk, and T. Tsuda (2009), Gravity wave and orographic wave activity observed around the Antarctic and Arctic stratospheric vortices by the COSMIC GPS-RO satellite constellation, *J. Geophys. Res.*, *114*, D17103, doi:10.1029/2009JD011851.

Alexander, S. P., A. R. Klekociuk, M. C. Pitts, A. J. McDonald, and A. Arevalo-Torres (2011), The effect of orographic gravity waves on Antarctic polar stratospheric cloud occurrence and composition, *J. Geophys. Res.*, *116*, D06109, doi:10.1029/2010JD015184.

Anthes, R. A. (2011), Exploring EarthŠs atmosphere with radio occultation: Contributions to weather, climate and space weather, *Atmos. Meas. Tech.*, *4*, 1077–1103.

Baines, P. G. (1995), *Topographic Effects in Stratified Fluids*, Cambridge Univ. Press, New York.

Baumgaertner, A., and A. McDonald (2007), A gravity wave climatology for Antarctica compiled from Challenging Minisatellite Payload/Global Positioning System (CHAMP/GPS) radio occultations, *J. Geophys. Res.*, *112*, D05103, doi:10.1029/2006JD007504.

Bilitza, D. (2002), Ionospheric models for radio propagation studies, in *Review of Radio Science 1999-2002*, edited by W. Ross Stone, pp. 625–679, Wiley, New York.

de la Torre, A., and P. Alexander (2005), Gravity waves above Andes detected from GPS radio occultation temperature profiles: Mountain forcing?, *Geophys. Res. Lett.*, *32*, L17815, doi:10.1029/2005GL022959.

de La Torre, A., A. Giraldez, and P. Alexander (1994), Saturated gravity wave spectra measured with balloons in Mendoza (Argentina), *Geophys. Res. Lett.*, *21*, 2039–2042.

de la Torre, A., P. Llamedo, P. Alexander, T. Schmidt, and J. Wickert (2010), Estimated errors in a global gravity wave climatology from GPS radio occultation temperature profiles, *Adv. Space Res.*, *46*, 174–179, doi:10.1016/j.asr.2010.02.033.

de la Torre, A., P. Alexander, P. Llamedo, R. Hierro, B. Nava, S. Radicella, T. Schmidt, and J. Wickert (2014), Wave activity at ionospheric heights above the Andes Mountains detected from FORMOSAT-3/COSMIC GPS radio occultation data, *J. Geophys. Res.*, *119*, 2046–2051, doi:10.1002/2013JA018870.

Fritts, D. C., and T. Lund (2011), Gravity wave influences in the thermosphere and ionosphere: Observations and modeling contributions, in *Aeronomy of the Earth's Atmosphere and Ionosphere*, edited by M. Abdu and D. Pancheva, pp. 109–130, Springer, Heidelberg.

Hamming, R. W. (1998), *Digital Filters*, 3rd ed., Dover Publ., Mineola, New York.

Hines, C. O. (1960), Internal atmospheric gravity waves at ionospheric heights, *Can. J. Phys.*, *38*, 1441–1481.

Hocke, K, and K Schlegel (1996), A review of atmospheric gravity waves and traveling ionospheric disturbances: 1982–1995, *Ann. Geophys.*, *14*, 917–940.

Hocke, K., and T. Tsuda (2001), Gravity waves and ionospheric irregularities over tropical convection zones observed by GPS/MET Radio Occultation, *Geophys. Res. Lett.*, *28*, 2815–2818.

Hocke, K., T. Tsuda, and A. de la Torre (2002), A study of stratospheric GW fluctuations and sporadic E at midlatitudes with focus on possible orographic effect of Andes, *J. Geophys. Res.*, *107*, 4428, doi:10.1029/2001JD001330.

Høeg, P., G. B. Larsen, H.-H. Benzon, J. Grove-Rasmussen, S. Syndergaard, M. D. Mortensen, J. Christensen, and K. Schultz, (1998), GPS atmosphere profiling methods and error assessments, Sci. Rep. 98-7, Sec. 4.1.4, Danish Meteorological Institute, Copenhagen, Denmark.

John, S. R., and K. K. Kumar (2012), TIMED/SABER observations of global gravity wave climatology and their interannual variability from stratosphere to mesosphere lower thermosphere, *Clim. Dyn.*, *39*, 1489–1505.

Kursinski, E. R., G. A. Hajj, J. T. Schofield, R. P. Linfield, and K. R. Hardy (1997), Observing Earth's atmosphere with radio occultation measurement using the Global Positioning System, *J. Geophys. Res.*, *102*, 23,429–23,465.

Lin, C. H., J. T. Lin, L. C. Chang, J. Y. Liu, C. H. Chen, W. H. Chen, H. H. Huang, and C. H. Liu (2012b), Observations of global ionospheric responses to the 2009 stratospheric sudden warming event by FORMOSAT-3/COSMIC, *J. Geophys. Res.*, *117*, A06323, doi:10.1029/2011JA017230.

Lin, C. H., J. T. Lin, L. C. Chang, W. H. Chen, C. H. Chen, and J. Y. Liu (2013), Stratospheric sudden warming effects on the ionospheric migrating tides during 2008–2010 observed by FORMOSAT-3/COSMIC, *J. Atmos. Sol. Terr. Phys.*, *103*, 66–75, doi:10.1016/j.jastp.2013.03.026.

Lin, J. T., C. H. Lin, L. C. Chang, H. H. Huang, J. Y. Liu, A. B. Chen, C. H. Chen, and C. H. Liu (2012a), Observational evidence of ionospheric migrating tide modification during the 2009 stratospheric sudden warming, *Geophys. Res. Lett.*, *39*, L02101, doi:10.1029/2011GL050248.

Liou, Y.-A., A. G. Pavelyev, S.-F. Liu, A. A. Pavelyev, N. Yen, C.-Y. Huang, and C.-J. Fong (2007), FORMOSAT-3/COSMIC GPS radio occultation mission: Preliminary results, *IEEE Trans. Geosci. Remote Sens.*, *45*, 3813–3826.

Llamedo, P., A. de la Torre, P. Alexander, D. Luna, T. Schmidt, and J. Wickert (2009), A gravity wave analysis near to the Andes Range from GPS radio occultation data and mesoscale numerical simulations: Two case studies, *Adv. Space Res.*, *44*, 494–500.

Luna, D., P. Alexander, and A. de la Torre (2013), Evaluation of uncertainty in gravity wave potential energy calculations through GPS radio occultation measurements, *Adv. Space Res.*, *52*, 879–882.

Lund, T. S., and D. C. Fritts (2012), Numerical simulation of gravity wave breaking in the lower thermosphere, *J. Geophys. Res.*, *117*, D21105, doi:10.1029/2012JD017536.

McDonald, A. J., B. Tan, and X. Chu (2010), Role of gravity waves in the spatial and temporal variability of stratospheric temperature measured by COSMIC/FORMOSAT-3 and Rayleigh lidar observations, *J. Geophys. Res.*, *115*, D19128, doi:10.1029/2009JD013658.

Mlynczak, M. G. (1997), Energetics of the mesosphere and lower thermosphere and the SABER experiment, *Adv. Space Res.*, *20*, 1177–1183.

Moffat-Griffin, T., M. J. Jarvis, S. R. Colwell, A. J. Kavanagh, G. L. Manney, and W. H. Daffer (2013), Seasonal variations in lower stratospheric gravity wave energy above the Falkland Islands, *J. Geophys. Res. Atmos.*, *118*, 10,861–10,869, doi:10.1002/jgrd.50859.

Park, J., H. Lühr, C. Lee, Y. H. Kim, G. Jee, and J.-H. Kim (2014), A climatology of medium-scale gravity wave activity in the midlatitude/low-latitude daytime upper thermosphere as observed by CHAMP, *J. Geophys. Res. Space Physics*, *119*, 2187–2196, doi:10.1002/2013JA019705.

Reisin, E. R., and J. Scheer (2004), Gravity wave activity in the mesopause region from airglow measurements at El Leoncito, *J. Atmos. Sol. Terr. Phys.*, *66*, 655–661.

Sato, K., S. Tateno, S. Watanabe, and Y. Kawatani (2012), Gravity wave characteristics in the Southern Hemisphere revealed by a high resolution middle atmosphere general circulation model, *J. Atmos. Sci.*, *69*, 1378–1396.

Schmidt, T., A. de la Torre, and J. Wickert (2008), Global gravity wave activity in the tropopause region from CHAMP radio occultation data, *Geophys. Res. Lett.*, *35*, L16807, doi:10.1029/2008GL034986.

Schreiner, W. S., S. V. Sokolovskiy, C. Rocken, and D. C. Hunt (1999), Analysis and validation of GPS/MET radio occultation data in the ionosphere, *Radio Sci.*, *34*, 949–966.

Smith, S., J. Baumgardner, and M. Mendillo (2009), Evidence of mesospheric gravity-waves generated by orographic forcing in the troposphere, *Geophys. Res. Lett.*, *36*, L08807, doi:10.1029/2008GL036936.

Tsuda, T., and K. Hocke (2004), Application of GPS radio occultation data for studies of atmospheric waves in the middle atmosphere and ionosphere, *J. Meteorol. Soc. Jpn.*, *82*, 419–426.

Vadas, S. L. (2007), Horizontal and vertical propagation and dissipation of gravity waves in the thermosphere from lower atmospheric and thermospheric sources, *J. Geophys. Res.*, *112*, A06305, doi:10.1029/2006JA011845.

Vadas, S. L., and H.-L. Liu (2013), The large-scale neutral and plasma responses to the body forces created by the dissipation of gravity waves from 6 hours of deep convection in Brazil, *J. Geophys. Res.*, *118*, 2593–2617, doi:10.1002/jgra.50249.

Vadas, S. L., D. C. Fritts, and M. J. Alexander (2003), Mechanism for the generation of secondary waves in wave breaking regions, *J. Atmos. Sci.*, *60*, 194–214.

Vadas, S. L., H.-L. Liu, and R. S. Lieberman (2014), Numerical modeling of the global changes to the thermosphere and ionosphere from the dissipation of gravity waves from deep convection, *J. Geophys. Res.*, *119*, 7762–7793, doi:10.1002/2014JA020280.

Wilson, R., M. L. Chanin, and A. Hauchecorne (1991), Gravity waves in the middle atmosphere observed by Rayleigh lidar 1. Case studies, *J. Geophys. Res.*, *96*, 5153–5167.

Yue, X., W. S. Schreiner, J. Lei, C. Rocken, D. C. Hunt, Y.-H. Kuo, and W. Wan (2010), Global ionospheric response observed by COSMIC satellites during the January 2009 stratospheric sudden warming event, *J. Geophys. Res.*, *115*, A00G09, doi:10.1029/2010JA015466.